Express Polymer Letters Vol.18, No.3 (2024) 282–295
Available online at www.expresspolymlett.com
https://doi.org/10.3144/expresspolymlett.2024.20

Research article

Preparation and characterization of Pickering foams by mechanical frothing and emulsion templating

Fatma Nur Parın[1*], *Hatice Dinç*[1], *Uğur Parın*[2], *Elife Kıldalı*[3], *Gökçe Taner*[3]

[1]Bursa Technical University, Faculty of Engineering and Natural Sciences, Department of Polymer Materials Engineering, 16310 Bursa, Turkey
[2]Aydın Adnan Menderes University, Faculty of Veterinary Medicine, Department of Microbiology, 09010 Aydın,Turkey
[3]Department of Bioengineering, Faculty of Engineering and Natural Sciences, Bursa Technical University, 16310 Bursa, Turkey

Received 27 September 2023; accepted in revised form 16 November 2023

Abstract. In this study, Pickering foamed emulsions have been prepared using β-cyclodextrin (β-CD), and *d*-limonene as a surfactant and an oil phase, respectively. The incorporation of β-CD/*d*-limonene inclusion complexes (ICs) in specific proportions (1:1, 1:3, and 1:5) to water phase, which is a polymer matrix composed of a mixture of polyvinyl alcohol (PVA) and psyllium husk (PSH) by mechanical frothing at high speed, and air bubbles have been formed in oil in water (o/w) emulsions. Ecofriendly bio-based foams have been developed in this method. Scanning Electron Microscope (SEM) analysis showed PVA/PSH Pickering foams usually open porous morphologies and the addition of *d*-limonene increases the amount of porosity from 43 to 49%. Although the resulting foams indicated similar thermal degradation profile, the presence of *d*-limonene in foams increased thermal stability. The surfaces of foams have a hydrophilic property with contact angles values lower than 80°. The tensile strength of foams decreased from 170 to 100 kPa due to the increased porosity. All foams indicated antibacterial activity to *Staphylococcus aureus* (*S. aureus*) with 9–12 mm zone inhibition. The incorporation of *d*-limonene into foams surprisingly decreased the cell viability. In brief, our findings show that the Pickering foams can be beneficial for wound healing applications.

Keywords: *Pickering foams, mechanical frothing, emulsion templating, polyvinyl alcohol (PVA), pysillium husk, β-CD/d-limonene inclusion complexes (ICs)*

1. Introduction

Foam and emulsion systems are all biphasic dispersions that consisting of two immiscible phases [1, 2]. These systems are thermodynamically unstable and require stabilization by surfactants [3]. A foam is a air-in-liquid dispersion, whereas an emulsion is a liquid-in-liquid dispersion [4]. Therefore, the surfactants can adsorb either the air–liquid interface or the liquid–liquid interface. On the other hand, foamed emulsions are oil, water, and air combinations [5]. A continuous phase of oil and water encloses the air bubbles. Foams are both due to the foaming ability of a liquid and it is responsible for the stability of the resulting foams. The inclusion of a third immiscible phase, such as oil into an aqueous foam or air into an emulsion, enhances opportunities of material design [5, 6]. Many studies have showed generally, water is used as continuous phase in most of the applications to obtain a foamed emulsion [7]. In these conventional foam or emulsion systems, stability has been satisfied by surfactants, however, these surfactants can damage the environment. Further, many of them have limited biocompatibility and toxicity, and easily affected by environmental factors [4, 8].

*Corresponding author, e-mail: nur.parin@btu.edu.tr

The major driving forces behind the creative development of biomass-based products are green chemistry and industrial ecology [9]. Moreover, bio-based and carbon-based biodegradable polymers such as cellulose, alginate, chitin, chitosan, and psyllium husk are significant options that might assist solve the ecological problem [10, 11]. Many studies have been conducted for different demands using these polymers such as heavy metal removal, wastewater purification, oil/water emulsion separation [12, 13].

As the requirement for renewable and environmentally friendly sustainable materials advances, many researchers have focused on particle-stabilized (or 'Pickering-Ramsden') emulsion or foams by using solid particles owing to lower cost, more reliable and safety in order to increase foam/emulsion stability [1, 14, 15].

Pickering emulsions or foams have previously been extensively utilized in pharmaceutical sciences, materials science, food science, biotechnology, and other fields [4, 16]. Pickering emulsions are regarded ideal for topical application to the skin and mucosal layers of the body [2, 17]. They are stabilized by various solid particles, particularly, inorganic-based such as silica, titanium dioxide, clay, hydroxyapatite, magnesium hydroxide. Nevertheless, such inorganic particles can be threat in terms of health. In this regard, many natural origin materials/biomacromolecules, polysaccharide-based solid particles like starch, cellulose, chitosan or other natural counterparts like protein can be used [2, 14, 15, 18]. The use of β-cyclodextrin (β-CD) as an emulsion stabilizer is another alternative for the production of Pickering emulsions. β-CD has hydrophobic inner cavity and hydrophilic outer cavity and can form non-covalent inclusion complexes (ICs) with oil and other guest molecules [19, 20].

Terpenes are natural substances composed of cycloaliphatic and/or aromatic compounds. *d*-limonene (4-isopropenyl-1-methylcyclohexene) is an essential part of several citrus-derived essential oils [21, 22]. It is regarded as a potential bioactive molecule due to its antibacterial, antioxidant, anticancer, anti-inflammatory, antiviral, and insecticidal properties.

In the current study, polyvinyl alcohol/psyllium husk (PVA/PSH) Pickering foamed emulsions containing *d*-limonene were produced by mechanical frothing. In this context, β-cyclodextrin/*d*-limonene ICs were prepared and added into PVA/PSH blend matrix and initiated high speed mixing. The effects of *d*-limonene on the morphological, physical, thermal, and mechanical properties of the material have been studied. Further, antibacterial and antifungal efficiency, and cytocompatibility assessment has been evaluated.

2. Materials and method

2.1. Materials

PVA (purity 87.8%, M_w ~30 000 g/mol) was purchased from ZAG Industrial Chemicals (Istanbul, Turkey). PSH powder was supplied from Naturebyme (İstanbul, Turkey). *d*-limonene (99% purity) were also purchased from Kimbiotek Chemical Substances Industry Trade Inc. (İstanbul, Turkey). β-CD was kindly granted by Wacker Chemical Company, Germany. Merck supplied Trypton Soy Agar (TSA, 105458) (Kirkland, QC, Canada). Further, RPMI1640 medium, fetal bovine serum (FBS), penicillin-streptomycin, 3-(4,5-dimethylthiazol-2-yl)-2,5-diphenyltetrazolium bromide (MTT), trypan blue, ethanol from Sigma; dimethyl sulfoxide (DMSO) from Merck; Triton X-100, trypsin–EDTA, Dulbecco's phosphate buffered saline (DPBS) from Gibco. Distilled water was used in all experiments, and all materials were utilized as received.

2.2. Fabrication of PVA/PSH/*d*-limonene Pickering foams

PVA powders were dissolved in distilled water at 90 °C to achieve homogenous 10% (w/v) PVA solutions. To obtain homogenous solution of psyllium husk (3%, w/v) the PSH solution was mixed with ultrasonic homogenizer for almost 1 h. Then, the PSH solution was taken and the PVA: PSH blend solution was started to be mixed in a mechanical mixer with a ratio of 4:1 (v/v). Thereafter, a certain amount of glycerol was added into the polymer mixture. After the addition of *d*-limonene to the system in different ratios (200, 600, and 1000 µL, respectively). *D*-limonene was added to the polymer mixture drop by drop. At the last step, physical crosslinker citric acid was added into polymer emulsions and mechanical frothing was applied these emulsions at high speed to obtain emulsion foams. These emulsion foams were transferred to teflon molds, and to obtain Pickering emulsion foams was taken to oven for drying at 50 °C for overnight. The sample codes were given as PPL0, PPL1, PPL2, and PPL3. The schematic sketch of preparation of PVA/PSH/*d*-limonene flexible foams were indicated in Figure 1. The foaming approach was used to create four bio-based

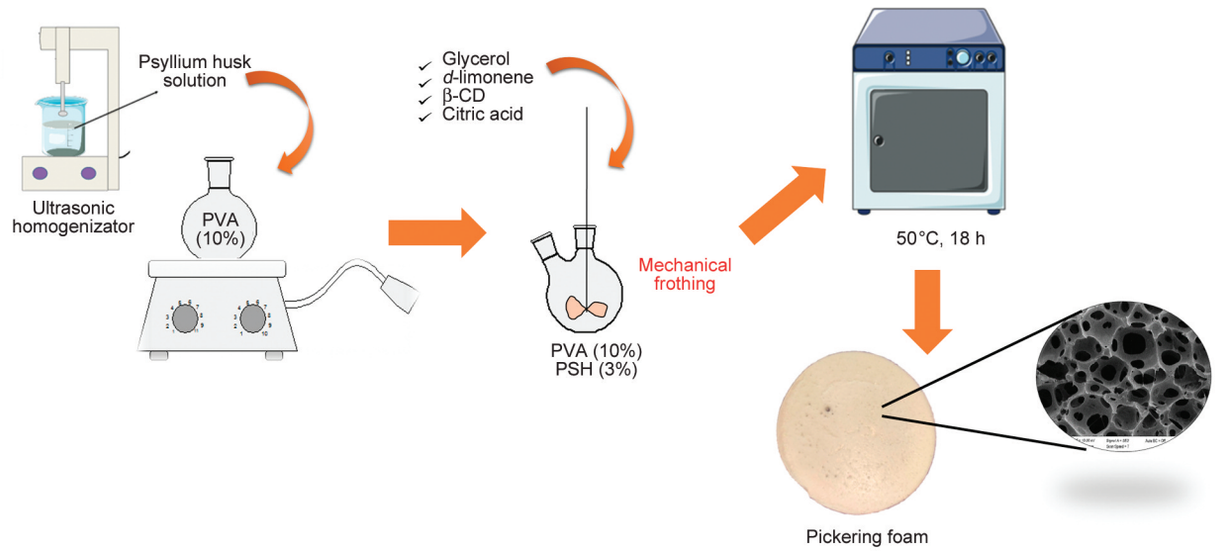

Figure 1. Schematic illustration of preparation of Pickering foams.

Table 1. The composition of PVA-PSH based samples.

Sample ID	PVA [% (w/v)]	PSH [% (w/v)]	Glycerol [% (v/v)]	β-cyclodextrin/*d*-limonene [% (w/v)]	Citric acid [% (w/w)]
PPL0	10	2	4	–	6
PPL1	10	2	4	1:1	6
PPL2	10	2	4	1:3	6
PPL3	10	2	4	1:5	6

materials formed of PVA/PSH film, and three different amounts of PVA/PSH/*d*-limonene foams (Table 1). In addition, step-by-step emulsion foam formation mechanism were given in Figure 2.

2.3. Characterization of the Foams

2.3.1. Morphological Analysis

The formation of the Pickering foams was observed with a stereo and light microscope (Leica-BM

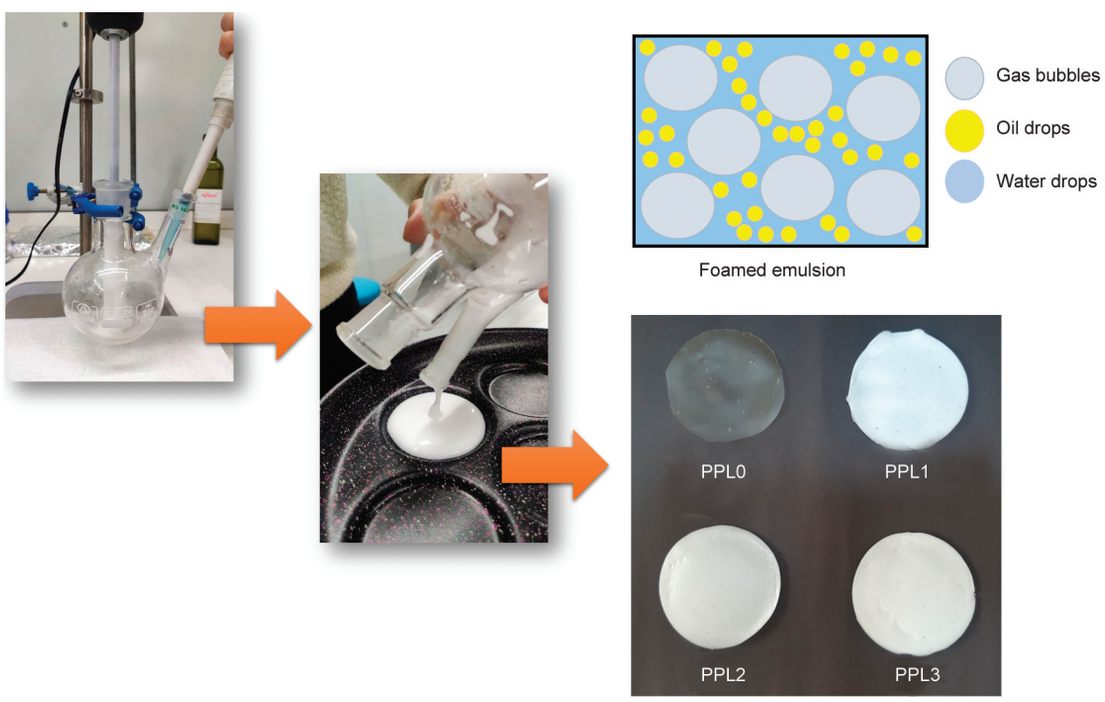

Figure 2. Step-by-step emulsion foam formation mechanism.

2500 M). The surface and cross-sectional morphologies of the samples produced was examined using a Carl Zeiss/Gemini 300 Scanning Electron Microscope (SEM). All samples were gold-coated in 15 nm before analysis. Porosity and pore diameters of the samples were measured via Image J (version 1.520 software) by randomly choosing 100 cavities for each sample.

2.3.2. Thermal stability

Thermogravimetric analysis (TGA) was carried out in a nitrogen atmosphere (N_2) at a heating rate of 10 °C/min over a temperature range of 30–600 °C, then in an oxygen atmosphere (O_2) at the same heating rate over a temperature range of 600–900 °C [15].

2.3.3. Spectroscopic analysis

Thermo Nicolet iS50 Fourier Transform Infrared (FT-IR) spectrometer (USA) with and ATR adaptor (Smart Orbit Diamond, USA) was utilized to confirm the chemical groups and interactions between polymer blends, and *d*-limonene – polymer blends in film, and foam samples. The analysis was performed in the wavenumber's region of 4000–500 cm^{-1} with an average 16 scans at 4 cm^{-1} resolution.

2.3.4. Wettability test

The wettability of resulting foams measured from a goniometer (Biolin Scientific, Gothenburg, Sweden), in the static contact angle method (sessile drop technique) which captured 15–20 records per second in standard mode for a single drop (3 µL pure water).

2.3.5. Mechanical test

The mechanical characteristics of the samples were tested by a universal testing machine (AGS-X Series, 1 kN, Shimadzu, Japan) in accordance with the modified ASTM D882-02 methodology. The samples were sliced into 5 cm long by 1.0 cm broad rectangles. The constant rate of deformation was 10 mm/min. The mechanical characteristics of each sample were investigated in terms of tensile strength, elongation at break, and Young's modulus using five repetitions. The data was provided as averages with standard deviations.

2.4. Antibacterial and antifungal test

The antibacterial sensitivities of hybrid non-wovens were determined by the standard strains of *Escherichia coli* ATCC® 25922, *Staphylococcus aureus* ATCC® 25923 and *Pseudomonas aeruginosa* ATCC® 27853. Trypton Soy Agar (Merck Millipore™ 105458) was used for the growth of lyophilized bacterial strains. The inoculated culture media were incubated for 24 h (37 °C) under aerobic condition. In an isotonic saline solution, bacterial suspensions were adjusted to 0.5 McFarland ($1 \cdot 10^8$ CFU/mL) turbidity. Antimicrobial efficacy was evaluated qualitatively by the disk diffusion method.

2.5. Cytocompatibility test

The cytocompatibility of developed biomaterials as a film sample, and 3 different foam samples prepared in different compositions was evaluated according to the ISO 1099-5 standard [23]. MTT cytotoxicity assay was performed in L929 cells after 24 h of exposure of cells to material extracts. Also the cytotoxic activity of *d*-limonene (known as citrus terpenes and is the main chemical constituent found in the cold-pressed peel oils that can be derived from all edible citrus species) which we used in the content of the material, was determined in a wide concentration range.

2.5.1. Preparation of biomaterial extract solutions

In this study in order to evaluate the cytocompability of PPL sample extracts, foremost all samples were cut as equal samples (2×2 cm) and sterilized by UV light for 1 h. Then they left for extraction for 24 h in sterile tubes containing 10mL of culture medium (RPMI 1640 containing 10% serum and 1% penicillin-streptomycin).

2.5.2. Cell culture

Cell culture and cytotoxicity assay were conducted at the bioengineering department of Bursa Technical University. The L929 fibroblast cell lines were used for cytotoxicity assays as a reference cell line for cytotoxicity testing of medical devices and materials. L929 cells were seeded in 75 cm^2 culture flasks containing RPMI 1640 supplemented with 10% FBS and 1% penicillin streptomycin. Cells were grown in an incubator at 37 °C in an atmosphere supplemented with 5% CO_2 and checked daily by using an inverted microscope with phase contrast attachment (Olympus CKX41). Subcultures were performed when an 80% of confluence was observed.

2.5.3. 3-(4,5-dimethylthiazol-2-yl)-2,5-diphenyltetrazolium bromide (MTT) assay

MTT assay was performed as detailed in our previous studies [24, 25]. A total of $5 \cdot 10^4$ cells/well were plated in 96 well tissue-culture plates and after 24 h incubation, cells were exposed to the 100 and 50% concentrations of sample's extract solutions for 24 h at 37 °C. The microscopical images of foams were given in Figure 3 and Figure 4, respectively. Then the medium was aspirated and MTT (5 mg/mL of stock in PBS) was added (10 µL/well in 100 µL of cell suspension), and cells were incubated for an additional 4 h with MTT dye. At the end of incubation period, the dye was carefully taken out and 100 µL of DMSO was added to each well. The absorbance of the solution in each well was measured in a microplate reader at 570 nm. Results were expressed as the average percentage of cell growth achieved from 8 wells replicated in each of two independent experiments.

3. Results and discussion

3.1. Stereo microscope and light microscope

The formation of the Pickering foams was observed with a stereo and light microscope [9]. The microscopical images of foams were given in Figure 3 and Figure 4, respectively.

3.2. Morphological analysis

SEM was used to analyze the surface and cross-sectional morphology of neat film and Pickering foams, and the resultant micrographs are shown in Figure 5. Further, pore sizes and pore size distributions were given in Figure 5. There are no irregularities in the SEM images of the PPL0 films as expected (Figure $5a_1$ and $5a_2$). The porous structure of foams dominates the cross-sectional and surface images. An increase in the amount of *d*-limonene has led to a decrease in pore diameters. This phenomenon coincides with the literature. Many studies reported that *d*-limonene provide extra hollowed ring morphology [26, 27]. β-cyclodextrin/*d*-limonene ICs

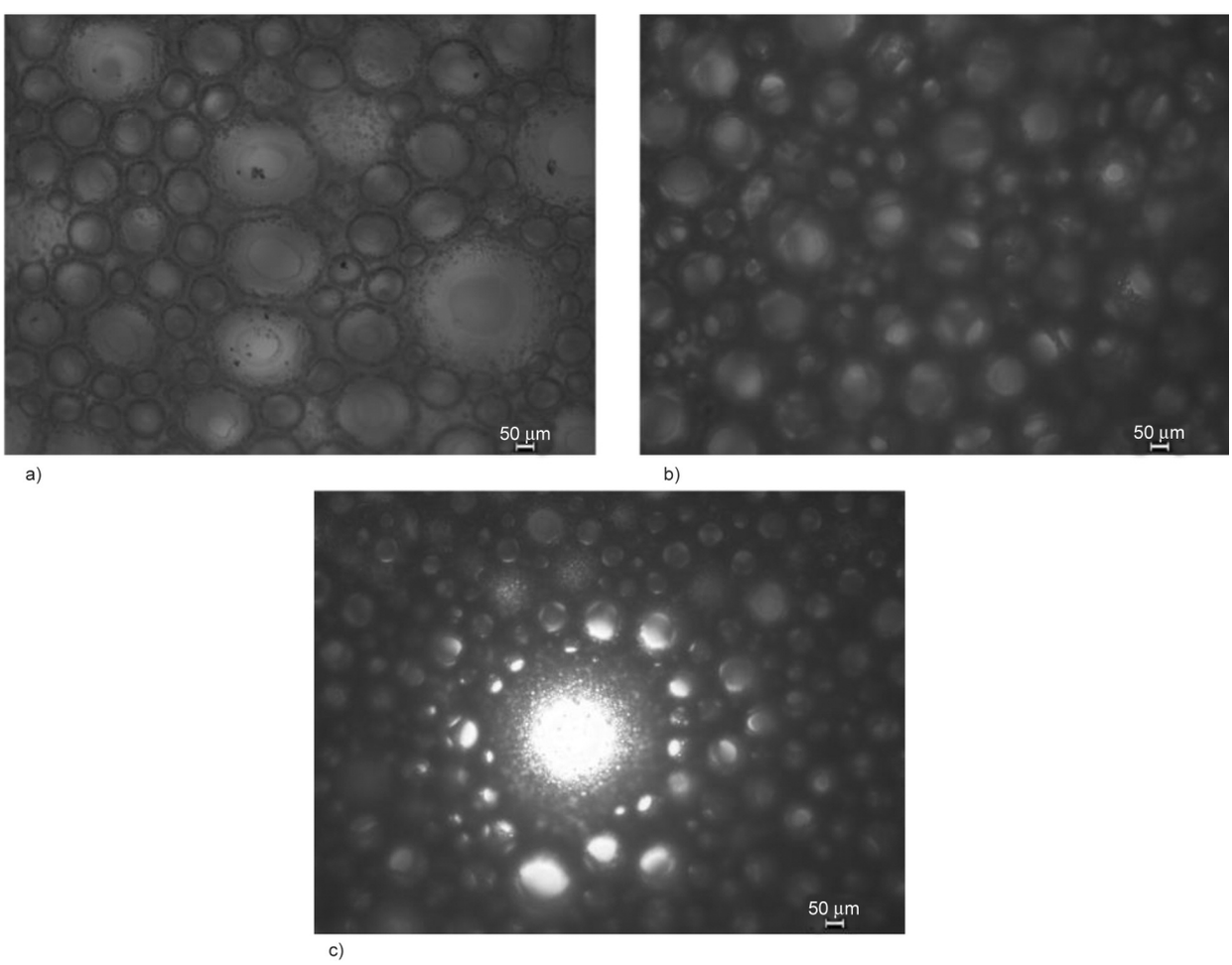

Figure 3. The light microscope images of the Pickering foams a) PPL1, b) PPL2, c) PPL3, respectively (Surface magnification: 100×, scale: 50 µm).

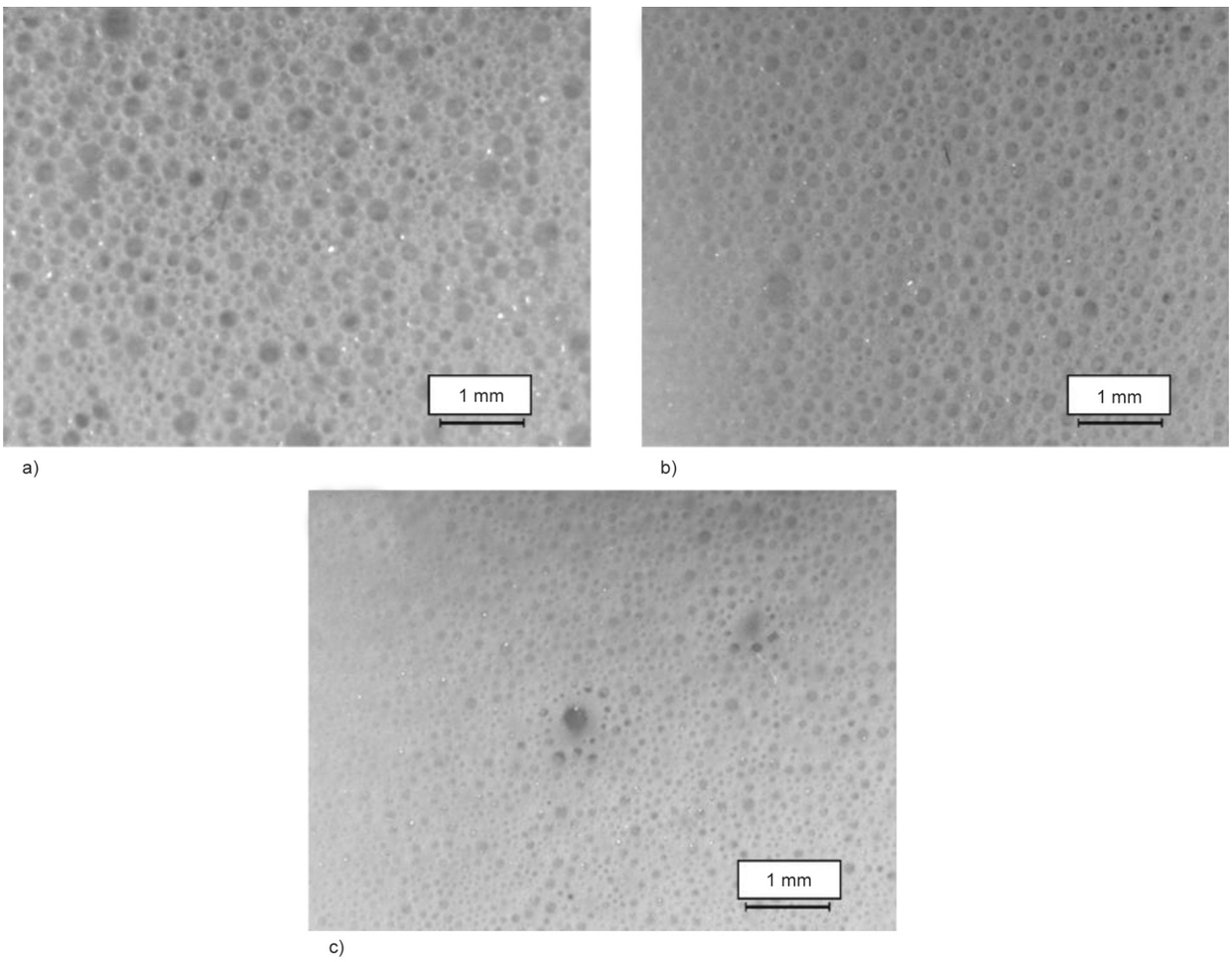

Figure 4. The stereo-microscope images of the Pickering foams a) PPL1, b) PPL2, c) PPL3, respectively (Surface magnification: 25×, scale: 1 mm).

were uniformly mixed in PVA/PSH matrix. However, uniformities of pore size distribution destroyed. The porosities of PPL1, PPL2, and PPL3 Pickering foams have been found as 43.4, 48.3, and 49.2%, respectively. Generally, open-cell morphology can be seen in all foams. Shapeless structures in the pore around are observed as the amount of *d*-limonene increases. Overall, the resulting Pickering foams were in the µm range with a 180–193 µm average pore diameter.

3.3. FT-IR spectrum

The FT-IR analysis was used to investigate to evaluate any bond formation of active ingredient and polymer. Further chemical groups of the polymers were confirmed (Figure 6). The spectra of pure PVA/PSH film, and PVA/PSH foams containing *d*-limonene show characteristic peaks of stretching and bending vibrations are due to the predominance of PVA an d PSH. In this context, the absorption peak at 3278 cm^{-1} is attributed to (–OH) stretching vibration. The asymmetric and symmetric stretching vibrations of the $–CH_2$ groups are due to the absorption bands at 2936, and 2913 cm^{-1}, respectively, as reported in previous studies [21, 28, 29]. Furthermore, the absorption peak at 1712 cm^{-1} revealed the existence of carbonyl groups (–C=O). This is owing to the esterification of PVAc. The consecutive peaks at 1420, 1374, 1321, and 1242 cm^{-1} are assigned to –CH and –OH groups bending (1374 cm^{-1}), O–H bending vibrations. It is noticeable from the spectra of all samples containing *d*-limonene foams that no chemical reaction occurs between *d*-limonene and PVA/PSH. When *d*-limonene was added in the PVA/PSH, slight changes were seen in the PPL2 foams spectra. Unlike the other samples, the PPL2 sample had a peak of 887 cm^{-1}. This can be attributable to an increase in *d*-limonene amount. Because this new peak formed is the characteristic peak of *d*-limonene (885 cm^{-1}). Furthermore, the amount of free *d*-limonene was observed at this point. The new peak The characteristic absorption peaks of *d*-limonene exhibited at 797 and

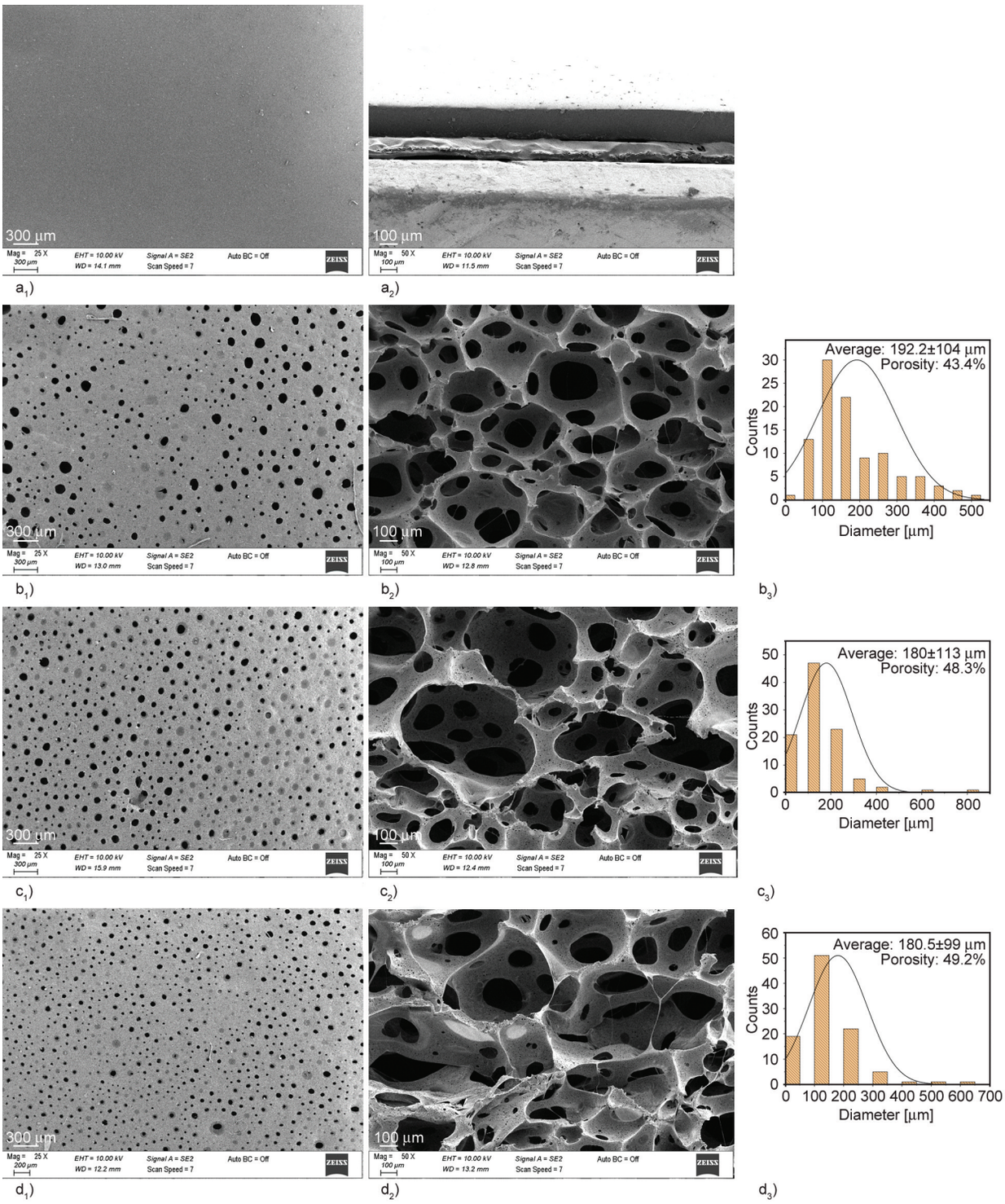

Figure 5. SEM surface images of samples a_1) PPL0, b_1) PPL1, c_1) PPL2, d_1) PPL3, cross-sectional images of foams a_2) PPL0, b_2) PPL1, c_2) PPL2, d_2) PPL3 and pore diameter of foams b_3) PPL1, c_3) PPL2, and d_3) PPL3, respectively. (Surface magnification: 25×, scale: 300 µm, and cross-sectional magnification: 50×, scale: 100 µm).

885 cm^{-1} owing to C–H bending, at 1639 cm^{-1} caused by C=C stretching, and 2964 and 2915 cm^{-1} due to C–H stretching.

3.4. Thermal properties

The thermal stability of the neat PVA/PSH film, and all foams were shown in Figure 7. In the first stage (30–100 °C), the excess moisture was vaporized for all samples. PPL0 and PPL1 samples indicated same degradation trend. According to TGA thermograms, the weight loss was occurred between (110–300 °C) due to the breakage of polymeric side chains and formation of a polyacetylene-like structure. In the third stage (300–400 °C), the breakage of polymer

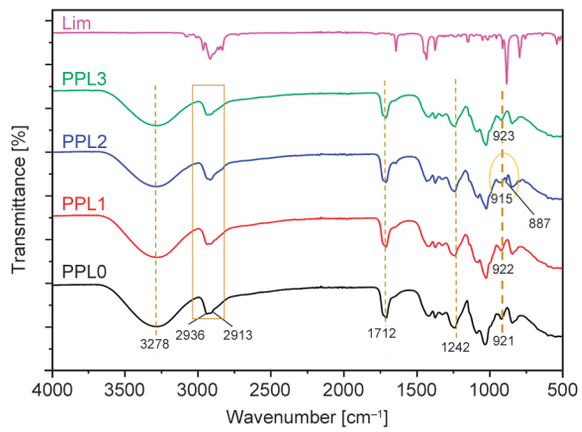

Figure 6. FT-IR spectra of the *d*-limonene, PPL0, PPL1, PPL2, and PPL3 samples.

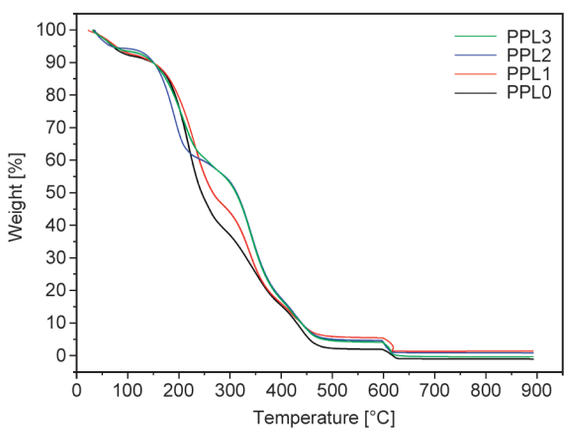

Figure 7. TGA thermograms of the neat PPL film ant flexible foams.

backbone (C–C and C–O bonds from PVA and PSH) arisen. In the fourth stage (400–600 °C), the formation of small molecules (CO_2, and CO *etc*.) was resulted from chain scission of PVA and polysaccharide degradation. In the last stage (after 600 °C), pyrolysis product and was decomposed [30].

The addition of *d*-limonene to the polymer matrix resulted in a slight rise in degradation temperatures. As incorporation of limonene in PVA/PSH matrix, the $T_{d_{50}}$ value of the films increased from 244 to 313 °C (Table 2). PPL2 and PPL3 foams have the highest thermal stability amongst the samples.

The TGA analysis was used to assess the thermal stability of the samples. Table 2 shows the TGA analysis results of all samples at 600 °C, including T_{onset}, $T_{d_{10}}$, $T_{d_{50}}$, $T_{d_{90}}$, and residual weight.

Table 2. Thermal properties of the samples.

Sample ID	$T_{d_{90}}$ [°C]	$T_{d_{50}}$ [°C]	$T_{d_{10}}$ [°C]	Residual weight [%]
PPL0	147.9	244.2	430.2	3.09
PPL1	148.7	266.6	439.0	1.38
PPL2	150.7	313.1	440.3	0.79
PPL3	149.1	311.6	439.2	2.46

3.5. Mechanical test

Mechanical strength of polymeric foams is significant criteria in both clinical and preclinical studies [21, 31] In this framework, a suitable dressing needs to be both flexible and durable [32]. On the other hand, porosity provides gas exchange, nutrition transfer, and enhance the absorption capacity of biomaterial. However, the existence of porosity often weakened the materials [33]. It is identified as a defect influencing the improvement of strength, as the failure stage is begun by the voids formed [34, 35].

The tensile strength of the PPL1, PPL2, and PPL3 foams were determined as 170±30, 100±20, and 100±30 kPa, while Young's modulus' were 200±80, 160±20, and 140±40 kPa, respectively (Table 3). This considerable changes in Young's modulus and percentage of elongation at max. break [%] values can be explained by variations in pore size [36]. While PPL1 foams could transfer stress uniformly, PPL2 and PPL3 foams may not distribute stress uniformly throughout the material because to varying pore size distributions, based on Image J data (Figure 2). Further, the increment of *d*-limonene content may cause decreasing of tensile strength values due to the plasticizing effect of oil-based *d*-limonene [21]. The incorporation of *d*-limonene in the foams resulted in an extra pore effect [26, 27]. This might also indicate that when the amount of oil in the foams increases, the elongation values do not rise as predicted. Overall, these bio-based materials possessed a foam-like structure and the formation of voids inside the composite, which function as a stress concentrator [15].

3.6. Wettability test

Some surface qualities must be satisfied to develop biologically safe biomaterials that come into contact with the human body. Critical interactions between tissue and substrate are influenced by many of factors,

Table 3. Mechanical properties of the samples.

Sample ID	Thickness [mm]	Tensile strength [kPa]	Young's modulus [kPa]	Max. elongation [%]
PPL0	0.46±0.15	4350±120	3820±18	527.43±119.8
PPL1	3.05±0.30	170±30	200±80	235.47±26.4
PPL2	3.78±0.48	100±20	160±20	167.24±30.7
PPL3	3.43±0.43	100±30	140±40	162.41±33.4

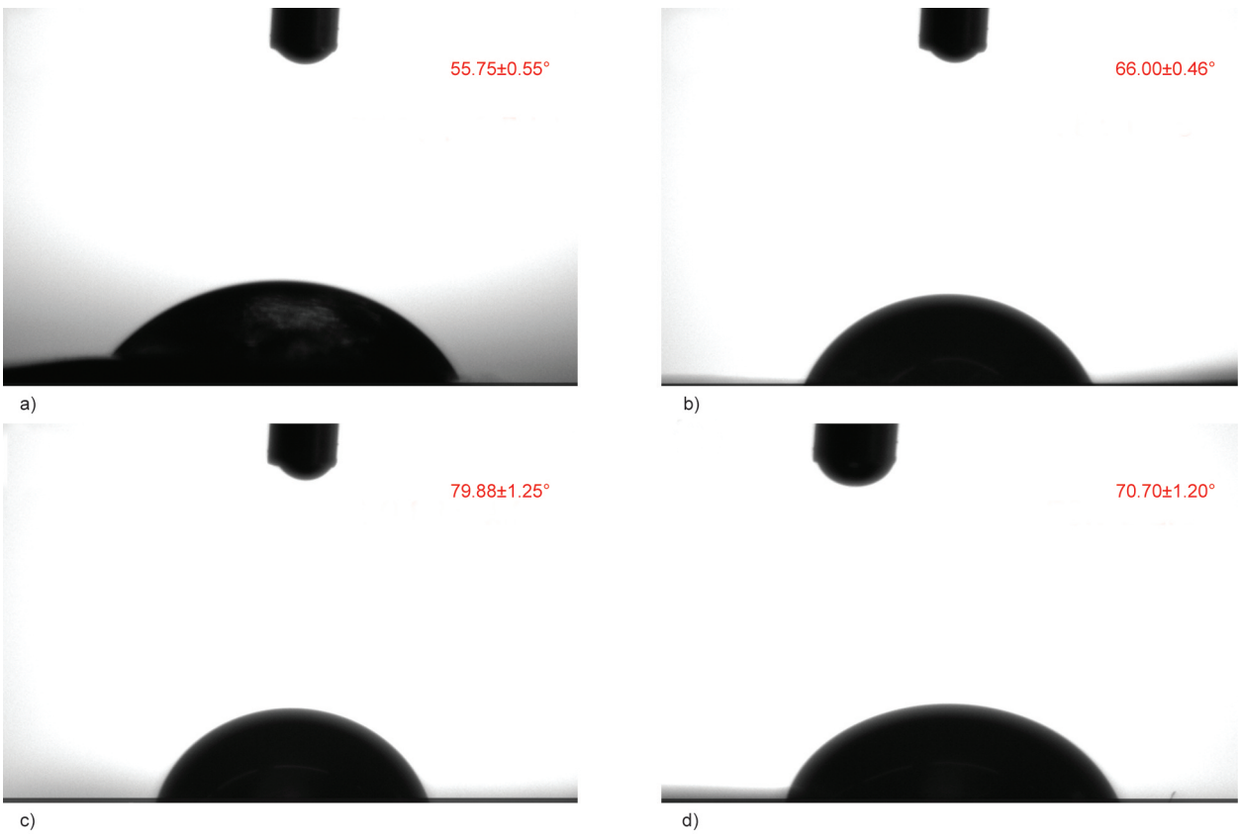

Figure 8. Contact angle values of the samples, a) PPL0, b) PPL1, c) PPL2, d) PPL3.

such as wettability, which has significant effects on biological reaction to biomaterial [37, 38]. The biomaterials should have hydrophilic characteristics to absorb a considerable amount of exudates [39] The surface wettability of the wound dressing is important when considering its function. Hydrophilic surfaces enhance cell attachment while hydrophobic surfaces provide adsorption. Moreover, during wound healing process, the wettability of the sample surface may be utilized to effect some cellular activities such as adhesion, cell proliferation, and *etc*. [40]. Wound dressings with improved wettability and moisture retention are favored for wound exudate control, whereas alternatives are required to assist dry wounds in retaining moisture. Surface of the biomaterials having contact angles below 90° are considered hydrophilic, in contrast those with contact angles above 90° are considered hydrophobic [14]. Herein, at time = 0, the contact angle result of PPL0 film' top surface was 55.75±0.75°. The incorporation of *d*-limonene leads to an increased hydrophobicity of surfaces (bigger contact angles) due to the hydrophobic properties of *d*-limonene with (value of log*P* = 4.38–4.8) [41–43]. In this case, the contact angle of PPL1, PPL2, and PPL3 increased with 66±0.46°, 79.88±1.2°, and 70.7±1.2°, respectively (Figure 8). However, it seems that the increase in these values is not correlated. This can be attributable to an inadequate binding between *d*-limonene and PVA/PSH polymer matrix (Figure 6) confirms that there is presence of free active substance (*d*-limonene) remaining on the foam surface.

3.7. Antibacterial and antifungal efficiency

Antibacterial and antifungal activity of PVA/PSH film, and *d*-limonene incorporated PVA/PSH foams was assessed against *E. coli*, *S. aureus*, and *C. albicans*, respectively (Figure 9).

The adhesive structure of PVA and PSH is used in wound treatment due to its bio-based and biocompatible properties. Many studies indicated hydrogel, fiber, membrane, scaffold, and foam forms of PVA and PSH are prepared for similar purposes [44–47]. Especially, PVA and carbohydrate-based PSH containing active substances in porous structure have properties such as biocompatibility, low toxicity, fluid absorption, high strength, and antibacterial activity. These properties also accelerate wound healing. Terpenes are natural substances that have been shown to have significant antibacterial activity against a variety of infections [48]. Terpene co-transport using matrices such as polymers decreases

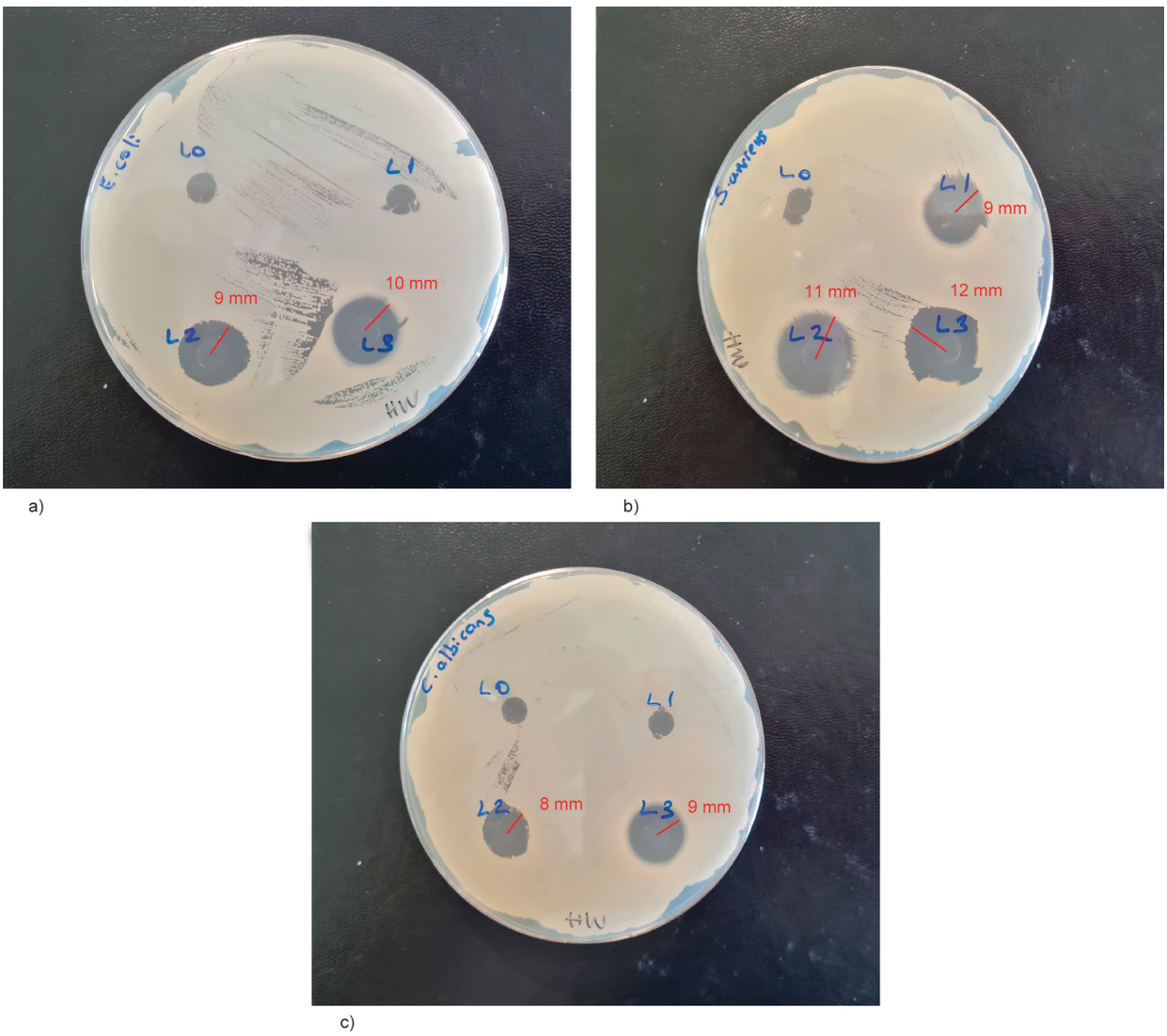

a) b) c)

Figure 9. Antibacterial activity of samples against a) *E. coli*, b) *S. aureus* and c) *C. albicans*, respectively.

terpene volatility while also limiting their detrimental impact from environmental impacts. *d*-limonene is one of the most abundant terpenes in nature [49]. Here, PVA/PSH foams containing *d*-limonene indicated good antibacterial activity. As amount of *d*-limonene rise in PVA/PSH foams, the foams demonstrated enhanced antibacterial efficiency for both Gram (–) and Gram (+) bacteria. However, PPL2 and PPL3 foams showed slightly less activity against Gram (–) bacteria compare to Gram (+) bacteria. Active substances utilize as antimicrobial agents by disrupting phospholipids in the cell membranes of bacteria, increasing permeability and cytoplasm leakage, or interacting with enzymes located on the cell wall [50]. It is known that Gram (–) bacteria have an external lipopolysaccharide membrane that surrounds the peptidoglycan cell wall [51]. Therefore, PPL2 and PPL3 foams have more antibacterial activity against *S. aerus* than *E. coli*. Further, PPL1 foams showed any activity to *E. coli*. This can be owing to the low concentration of *d*-limonene in the foams, and also the small amount of foams used during antibacterial test [52]. Additionally, it is reported *d*-limonene loaded-PVP/PAAm hydrogels does not show any antibacterial activity to *E. coli* and *S. aeurus* bacteria [14]. This may also be due to the fact that the final materials do not contain an amount of active substances that can have an antibacterial effect. Moreover, the existence of beta-cyclodextrin in the foams may have increased the antibacterial activity of the materials. Although this phenomenon has not been verified in a study performed by Estevez-Areco *et al*. [52] it has been demonstrated that *R*-limonene encapsulation increases and its volatility reduces. This may indicate that the release of *d*-limonene from the foam may be difficult due to the formation of a good β-CD/*d*-limonene inclusion complex.

3.8. Cytotoxic effects of materials by MTT assay

The cytotoxic effect of the extract solutions of different PPL samples was evaluated by MTT assay in L929 cells. Untreated negative control group and positive control group with Triton x-100 were also evaluated. The average absorbance values and standard deviation values of living cells were calculated by averaging all the data obtained. In addition, cell viability in the untreated control group was considered as 50%, and living cell percentages were determined for all samples compared to the control. Results of MTT test are shown in Figure 10. According 50% extracts of PPL0 and PPL1 did not show any cytotoxic effects, on the contrary, they promoted proliferation and caused an increase in cell viability. PPL3 samples caused some decreases in cell viability compared to the negative control group. However, it should be noted that these tests have been carried out with extract solutions of materials prepared under extreme conditions in terms of quantity and cannot have this effect in contact toxicity.

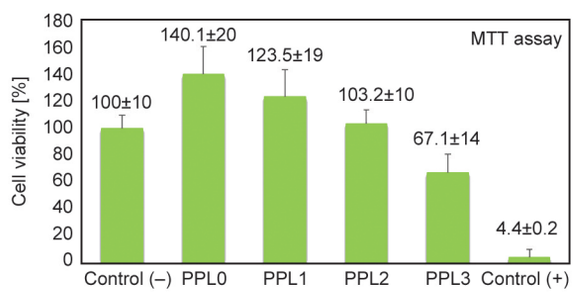

Figure 10. Effects of PPL extract solutions on cell viability of L929 cells by MTT assay. Results were expressed as the mean percentage of cell growth inhibition from 3 independent experiments. Cell viability was plotted as percent of control (assuming data obtained from the absence of materials as 100%).

In this study, *d*-limonene was also tested alone in a wide range of concentrations (0.008–0.5%) to determine the cytotoxicity profile. The results are given in Figure 11. According to the results *d*-limonene caused a decrease in cell viability only at the highest concentrations (0.5 and 1%).

Shah *et al*. [53] researched on *in vitro* and *in vivo* effect of *d*-limonene on primary hepatocytes and K562 tumor implanted C57BL/6 mice. MTT results showed that *d*-limonene has no cytotoxic effect on normal primary hepatocytes at tested concentrations (1, 2, 4 and 8 mM). According to the *in vivo* studies on on K562 tumor implanted C57BL/6 mice, *d*-limonene leads the regression of tumor growth.

In order to evaluate the cytotoxic activity on *d*-limonen-loaded niosomes, Hajizadeh *et al*. [54] used HepG2, MCF-7, and A549 cell lines. *d*-limonene-loaded niosomes showed cytotoxic effect on all cancer cell lines. These results showed that niosome loaded with phytochemicals can be potential nanocarier for cancer therapy.

4. Conclusions

Bio-based Pickering foams were produced using β-CD which is known polysaccharide based surfactant. During the process, air bubbles were formed in o/w emulsions by applying high mechanical speed

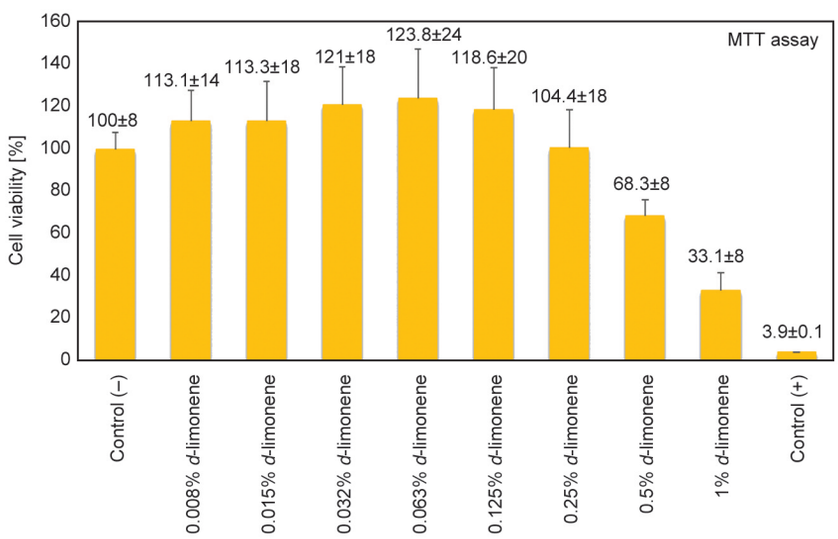

Figure 11. Effects of *d*-limonene on cell viability of L929 cells by MTT assay. Results were expressed as the mean percentage of cell growth inhibition from 3 independent experiments. Cell viability was plotted as percent of control (assuming data obtained from the absence of materials as 100%).

mixing to o/w emulsions. While morphological, thermal, and wettability properties and antibacterial activities of the resulting foams were improved by the addition of *d*-limonene, mechanical properties and biocompatibility assessments were partially negative affected. In general, the values of the PPL2 foams with β-CD/*d*-limonene ratio of (1:3, w/v) are the best in light of all of the results. Consequently, the obtained Pickering foams can be good candidates to use in wound healing applications.

Acknowledgements

The authors would like to thank Aycan Altun for her kind help in the contact angle measurements and Bursa Technical University Chemical Engineering Department.
This study was financially supported by TUBITAK within the scope of the 2209-A project (Project number: 1919B012110054).

References

[1] Lam S., Velikov K. P., Velev O. D.: Pickering stabilization of foams and emulsions with particles of biological origin. Current Opinion in Colloid and Interface Science, **19**, 490–500 (2014). https://doi.org/10.1016/j.cocis.2014.07.003

[2] Jug M., Yoon B. K., Jackman J. A.: Cyclodextrin-based Pickering emulsions: Functional properties and drug delivery applications. Journal of Inclusion Phenomena and Macrocyclic Chemistry, **101**, 31–50 (2021). https://doi.org/10.1007/s10847-021-01097-z

[3] Liu C., Tian Y., Ma Z., Zhou L.: Pickering emulsion stabilized by β-cyclodextrin and cinnamaldehyde/β-Cyclodextrin composite. Foods, **12**, 2366 (2023). https://doi.org/10.3390/foods12122366

[4] Zhu Y., Wang A.: Pickering emulsions and foams stabilization based on clay minerals. in 'Developments in Clay Science' (eds.: Wypych F., de Freitas R. A.) Elsevier, Amsterdam, Vol. 10, 169–227 (2022). https://doi.org/10.1016/B978-0-323-91858-9.00001-X

[5] Salonen A.: Mixing bubbles and drops to make foamed emulsions. Current Opinion in Colloid and Interface Science, **50**, 101381 (2020). https://doi.org/10.1016/j.cocis.2020.08.006

[6] Brun M., Delample M., Harte E., Lecomte S., Leal-Calderon F.: Stabilization of air bubbles in oil by surfactant crystals: A route to produce air-in-oil foams and air-in-oil-in-water emulsions. Food Research International, **67**, 366–375 (2015). https://doi.org/10.1016/j.foodres.2014.11.044

[7] Dinache A., Pascu M-L., Smarandache A.: Spectral properties of foams and emulsions. Molecules, **26**, 7704 (2021). https://doi.org/10.3390/molecules26247704

[8] Mwangi W. W., Lim H. P., Low L. E., Tey B. T., Chan E. S.: Food-grade Pickering emulsions for encapsulation and delivery of bioactives. Trends in Food Science and Technology, **100**, 320–332 (2020). https://doi.org/10.1016/j.tifs.2020.04.020

[9] An C., Zhang M., Xiao Z., Yang Q., Feng L., Li S., Shi M.: Lignocellulose/chitosan hybrid aerogel composited with fluorescence molecular probe for simultaneous adsorption and detection of heavy metal pollutants. Journal of Environmental Chemical Engineering, **11**, 111205 (2023). https://doi.org/10.1016/j.jece.2023.111205

[10] Zhang M., Shi Y., Wang R., Chen K., Zhou N., Yang Q., Shi J.: Triple-functional lignocellulose/chitosan/Ag@TiO_2 nanocomposite membrane for simultaneous sterilization, oil/water emulsion separation, and organic pollutant removal. Journal of Environmental Chemical Engineering, **9**, 106728 (2021). https://doi.org/10.1016/j.jece.2021.106728

[11] Zhang M., Shi L., Du X., Li Z., Shi Y., An C., Li J., Wang C., Shi J.: Janus mesoporous wood-based membrane for simultaneous oil/water separation, aromatic dyes removal, and seawater desalination. Industrial Crops and Products, **188**, 115643 (2022). https://doi.org/10.1016/j.indcrop.2022.115643

[12] Zhang M., Zhou N., Shi Y., Ma Y., An C., Li J., Jiang W., Wang C., Shi J.: Construction of antibacterial, superwetting, catalytic, and porous lignocellulosic nanofibril composites for wastewater purification. Advanced Materials Interfaces, **9**, 2201388 (2022). https://doi.org/10.1002/admi.202201388

[13] Zhang M., Wang C., Ma Y., Du X., Shi Y., Li J., Shi J.: Fabrication of superwetting, antimicrobial and conductive fibrous membranes for removing/collecting oil contaminants. RSC advances, **10**, 21636–21642 (2020). https://doi.org/10.1039/d0ra02704a

[14] Parın F. N.: A green approach to the development of novel antibacterial cinnamon oil loaded-PVA/egg white foams *via* Pickering emulsions. Journal of Porous Materials, **30**, 1233–1243 (2023). https://doi.org/10.1007/s10934-022-01417-9

[15] Parin F. N., Deveci S.: Production and characterization of bio-based sponges reinforced with hypericum perforatum oil (St. John's Wort Oil) *via* pickering emulsions for wound healing applications. ChemistrySelect, **8**, e202203692 (2023). https://doi.org/10.1002/slct.202203692

[16] Denkov N., Tcholakova S., Cholakova D.: Surface phase transitions in foams and emulsions. Current Opinion in Colloid and Interface Science, **44**, 32–47 (2019). https://doi.org/10.1016/j.cocis.2019.09.005

[17] Marto J., Ascenso A., Simoes S., Almeida A. J., Ribeiro H. M.: Pickering emulsions: Challenges and opportunities in topical delivery. Expert Opinion on Drug Delivery, **13**, 1093–1107 (2016). https://doi.org/10.1080/17425247.2016.1182489

[18] Choi S-J., Lee J. K., Jeong J., Choy J-H.: Toxicity evaluation of inorganic nanoparticles: Considerations and challenges. Molecular and Cellular Toxicology, **9**, 205–210 (2013). https://doi.org/10.1007/s13273-013-0026-z

[19] Li C., Luo X., Li L., Cai Y., Kang X., Li P.: Carboxymethyl chitosan-based electrospun nanofibers with high citral-loading for potential anti–infection wound dressings. International Journal of Biological Macromolecules, **209**, 344–355 (2022). https://doi.org/10.1016/j.ijbiomac.2022.04.025

[20] Kundu M., Saha S., Roy M. N.: Evidences for complexations of β-cyclodextrin with some amino acids by ^{1}H NMR, surface tension, volumetric investigations and XRD. Journal of Molecular Liquids, **240**, 570–577 (2017). https://doi.org/10.1016/j.molliq.2017.05.123

[21] Parın F. N., Ullah A., Yeşilyurt A., Parın U., Haider M. K., Kharaghani D.: Development of PVA–psyllium husk meshes *via* emulsion electrospinning: Preparation, characterization, and antibacterial activity. Polymers, **14**, 1490 (2022). https://doi.org/10.3390/polym14071490

[22] Masood A., Ahmed N., Razip Wee M. M., Patra A., Mahmoudi E., Siow K. S.: Atmospheric pressure plasma polymerisation of *D*-limonene and its antimicrobial activity. Polymers, **15**, 307 (2023). https://doi.org/10.3390/polym15020307

[23] UNI EN ISO 10993-5: Biological evaluation of medical devices – Part 5: In vitro cytotoxicity testing (2009).

[24] Parın F. N., Aydemir Ç. İ., Taner G., Yıldırım K.: *Co*-electrospun-electrosprayed PVA/folic acid nanofibers for transdermal drug delivery: Preparation, characterization, and *in vitro* cytocompatibility. Journal of Industrial Textiles, **51**, 1323S–1347S (2022). https://doi.org/10.1177/1528083721997185

[25] Parın F. N., Yıldırım K., Taner G., Kıldalı E.: Development and characterization of vitamin B9 – Electrosprayed non-woven surfaces for wound healing applications. Eskişehir Technical University Journal of Science and Technology A: Applied Sciences and Engineering, **22**, 70–84 (2021). https://doi.org/10.18038/estubtda.983329

[26] Kekevi B.: Synthesis and characterization of bio-derived monoliths. Bilecik Şeyh Edebali Üniversitesi Fen Bilimleri Dergisi, **8**, 826–832 (2021). https://doi.org/10.35193/bseufbd.963141

[27] Parın F. N.: Synthesis and characterisation of PVP-AAm hydrogels *via* hybrid process: Morphological, physical, and antibacterial activity. Journal of Advanced Research in natural and Applied Sciences, **9**, 697–709 (2023). https://doi.org/10.28979/jarnas.1255113

[28] Lan W., Liang X., Lan W., Ahmed S., Liu Y., Qin W.: Electrospun polyvinyl alcohol/*D*-limonene fibers prepared by ultrasonic processing for antibacterial active packaging material. Molecules, **24**, 4286 (2019). https://doi.org/10.3390/molecules24040767

[29] Kumar D., Pandey J., Kumar P., Raj V.: Psyllium mucilage and its use in pharmaceutical field: An overview. Current Synthetic Systems Biology, **5**, 134 (2017). https://doi.org/10.4172/2332-0737.1000134

[30] Sharma V. K., Mazumder B.: Crosslinking of Isabgol husk polysaccharides for microspheres development and its impact on particle size, swelling kinetics and thermal behavior. Polymer Bulletin, **71**, 735–757 (2014). https://doi.org/10.1007/s00289-013-1089-7

[31] Wang L., Wang C., Wu S., Fan Y., Li X.: Influence of the mechanical properties of biomaterials on degradability, cell behaviors and signaling pathways: Current progress and challenges. Biomaterials Science, **8**, 2714–2733 (2020). https://doi.org/10.1039/d0bm00269k

[32] Kiran A. S. K., Ramakrishna S.: Biomaterials: Basic principles. in 'An introduction to biomaterials science and engineering' (eds.: Kiran A. S. K., Ramakrishna S.) World Scientific, Singapore, 82–93 (2021). https://doi.org/10.1142/9789811228186_0004

[33] Bonvallet P. P., Culpepper B. K., Bain J. L., Schultz M. J., Thomas S. J., Bellis S. L.: Microporous dermal-like electrospun scaffolds promote accelerated skin regeneration. Tissue Engineering Part A, **20**, 2434–2445 (2014). https://doi.org/10.1089/ten.tea.2013.0645

[34] Al-Maharma A. Y., Patil S. P., Markert B.: Effects of porosity on the mechanical properties of additively manufactured components: A critical review. Materials Research Express, **7**, 122001 (2020). https://doi.org/10.1088/2053-1591/abcc5d

[35] Gasti T., Dixit S., Hiremani V. D., Chougale R. B., Masti S. P., Vootla S. K., Mudigoudra B. S.: Chitosan/pullulan based films incorporated with clove essential oil loaded chitosan-ZnO hybrid nanoparticles for active food packaging. Carbohydrate Polymers, **277**, 118866 (2022). https://doi.org/10.1016/j.carbpol.2021.118866

[36] Parın F. N., Mert E. H.: Hydrophilic closed-cell macroporous foam preparation by emulsion templating. Materials Letters, **277**, 128287 (2020). https://doi.org/10.1016/j.matlet.2020.128287

[37] Agrawal G., Negi Y. S., Pradhan S., Dash M., Samal S. K.: Wettability and contact angle of polymeric biomaterials. in 'Characterization of polymeric biomaterials' (eds.: Tanzi M. C., Faré S.) Woodhead, Sawston, 57–81 (2017). https://doi.org/10.1016/B978-0-08-100737-2.00003-0

[38] Kazimierczak P., Benko A., Nocun M., Przekora A.: Novel chitosan/agarose/hydroxyapatite nanocomposite scaffold for bone tissue engineering applications: Comprehensive evaluation of biocompatibility and osteoinductivity with the use of osteoblasts and mesenchymal stem cells. International Journal of Nanomedicine, **14**, 6615–6630 (2019). https://doi.org/10.2147/IJN.S217245

[39] Vivcharenko V., Wojcik M., Palka K., Przekora A.: Highly porous and superabsorbent biomaterial made of marine-derived polysaccharides and ascorbic acid as an optimal dressing for exuding wound management. Materials, **14**, 1211 (2021). https://doi.org/10.3390/ma14051211

[40] Mohsen A. H., Ali N. A.: Improve wettability of polycaprolactone (PCL)/chitosan of wound dressings by plasma jet. Iraqi Journal of Science, **63**, 4761–4770 (2022). https://doi.org/10.24996/ijs.2022.63.11.15

[41] Feng J., Wang R., Chen Z., Zhang S., Yuan S., Cao H., Jafari S. M., Yang W.: Formulation optimization of *D*-limonene-loaded nanoemulsions as a natural and efficient biopesticide. Colloids and Surfaces A: Physicochemical and Engineering Aspects, **596**, 124746 (2020). https://doi.org/10.1016/j.colsurfa.2020.124746

[42] Marcuzzo E., Debeaufort F., Sensidoni A., Tat L., Beney L., Hambleton A., Pressini D., Voilley A.: Release behavior and stability of encapsulated *D*-limonene from emulsion-based edible films. Journal of Agricultural and Food Chemistry, **60**, 12177–12185 (2012). https://doi.org/10.1021/jf303327n

[43] El-Deen A. K., Shimizu K.: Application of *D*-limonene as a bio-based solvent in low density-dispersive liquid–liquid microextraction of acidic drugs from aqueous samples. Analytical Sciences, **35**, 1385–1391 (2019). https://doi.org/10.2116/analsci.19P360

[44] Gundu S., Sahi A. K., Varshney N., Varghese J., K. Vishwakarma N., Mahto S. K.: Fabrication and *in vitro* characterization of luffa-based composite scaffolds incorporated with gelatin, hydroxyapatite and psyllium husk for bone tissue engineering. Journal of Biomaterials Science, Polymer Edition, **33**, 2220–2248 (2022). https://doi.org/10.1080/09205063.2022.2101415

[45] Pattnayak B. C., Mohapatra S.: Multifunctional biobased photothermal hydrogel for highly efficient seawater desalination and contaminant adsorption. Journal of Environmental Chemical Engineering, **10**, 108616 (2022). https://doi.org/10.1016/j.jece.2022.108616

[46] Tamer T. M., Sabet M. M., Omer A. M., Abbas E., Eid A. I., Mohy-Eldin M. S., Hassan M. A.: Hemostatic and antibacterial PVA/kaolin composite sponges loaded with penicillin–streptomycin for wound dressing applications. Scientific Reports, **11**, 3428 (2021). https://doi.org/10.1038/s41598-021-82963-1

[47] Singh B., Sharma V.: Design of psyllium–PVA–acrylic acid based novel hydrogels for use in antibiotic drug delivery. International Journal of Pharmaceutics, **389**, 94–106 (2010). https://doi.org/10.1016/j.ijpharm.2010.01.022

[48] Álvarez-Martínez F. J., Barrajón-Catalán E., Herranz-López M., Micol V.: Antibacterial plant compounds, extracts and essential oils: An updated review on their effects and putative mechanisms of action. Phytomedicine, **90**, 153626 (2021). https://doi.org/10.1016/j.phymed.2021.153626

[49] Han Y., Sun Z., Chen W.: Antimicrobial susceptibility and antibacterial mechanism of limonene against *Listeria monocytogenes*. Molecules, **25**, 33 (2019). https://doi.org/10.3390/molecules25010033

[50] Trombetta D., Castelli F., Sarpietro M. G., Venuti V., Cristani M., Daniele C., Saija A., Mazzanti G., Bisignano G.: Mechanisms of antibacterial action of three monoterpenes. Antimicrobial Agents and Chemotherapy, **49**, 2474–2478 (2005). https://doi.org/10.1128/aac.49.6.2474-2478.2005

[51] Silhavy T. J., Kahne D., Walker S.: The bacterial cell envelope. Cold Spring Harbor Perspectives in Biology, **2**, a000414 (2010). https://doi.org/10.1101/cshperspect.a000414

[52] Estevez-Areco S., Guz L., Candal R., Goyanes S.: Development of insoluble PVA electrospun nanofibers incorporating R-limonene or β-cyclodextrin/R-limonene inclusion complexes. Journal of Polymers and the Environment, **30**, 2812–2823 (2022). https://doi.org/10.1007/s10924-022-02390-9

[53] Shah B., Shaikh M. V., Chaudagar K., Nivsarkar M., Mehta A.: *D*-limonene possesses cytotoxicity to tumor cells but not to hepatocytes. Polish Annals of Medicine, **26**, 98–104 (2019). https://doi.org/10.29089/2017.17.00047

[54] Hajizadeh M. R., Maleki H., Barani M., Fahmidehkar M. A., Mahmoodi M., Torkzadeh-Mahani M.: *In vitro* cytotoxicity assay of *D*-limonene niosomes: An efficient nano-carrier for enhancing solubility of plant-extracted agents. Research in Pharmeceutical Sciences, **14**, 448–458 (2019). https://doi.org/10.4103/1735-5362.268206